Carrier-stabilized hexagonal Ge

Xuefen Cai [1] Hui-Xiong Deng [2,*] and Su-Huai Wei [1,†]

[1] *Beijing Computational Science Research Center, Beijing 100193, China*
[2] *State Key Laboratory of Superlattices and Microstructures, Institute of Semiconductors, Chinese Academy of Sciences, Beijing 100083, China*

Germanium is crystalized in the cubic diamond structure, but its high energy hexagonal Ge (lonsdaleite) phase has many novel properties such as direct band gap. Using first-principles calculations, we show that the hexagonal lonsdaleite phase of Ge can be stabilized by introducing carriers, either electrons or holes, because Ge in the cubic and hexagonal phases form a type-I band alignment with both electrons and holes localized at the hexagonal site. This result is distinct from that in zinc-blende compounds such as ZnSe, because due to the lack of inversion symmetry, the crystal-field splitting, zone folding, and symmetry-controlled level repulsion between valence and conduction band states lead to a type-II band alignment between its cubic and hexagonal phases, so the hexagonal (wurtzite) phase of ZnSe can only be stabilized, in principle, by holes. This distinction reveals that, due to the symmetry differences, the well-investigated understanding of band structure differences between zinc-blende and wurtzite phases should not be simply extended to that of diamond and lonsdaleite phases despite the remarkable structure resemblance between the two cases.

I. INTRODUCTION

Classic group-IV elemental semiconductors Si and Ge undoubtedly take on the key roles in electronic and information industries [1,2]. Unfortunately, they exhibit the indirect band gap when they crystalize in their ground state cubic diamond structure, which has hindered their application in optoelectronic devices. Interestingly, the metastable hexagonal lonsdaleite Ge [3] is expected to be a direct band gap semiconductor [4,5] and indeed a recent work by Fadaly *et al.* [6] has shown that it is able to generate an emission comparable to that of the group III–V compounds with direct band gap. As a result, a thorough knowledge of the band structure of lonsdaleite Ge and its relationship with its cubic phase is of great significance. Despite that several theoretical studies on Ge have offered valuable information on its electronic and optical properties [4,5,7], the relationship between the electronic band structures of the hexagonal Ge phase and the ground state cubic phase and their stability still remain elusive.

It is known that the lonsdaleite phase has analogous local atomic environments with the diamond one. The two differ from each other by the different stacking arrangement of the hexagon atomic layers: cubic structure displays a stacking sequence of *ABCABC...* in the (111) direction, whereas the hexagonal phase shows a stacking type of *ABAB...* along the (0001) direction. Actually, the same arrangements occur in the zinc-blende and wurtzite structures [8], which can be respectively perceived as the diamond and lonsdaleite structures containing two different components, thus lacking the inversion symmetry. As a convention, the diamond and zinc-blende structures could be referred to as 3*C* cubic phases, while both lonsdaleite and wurtzite structures can be designated as

2*H* hexagonal phases. Indeed, the relationship between the electronic properties in the binary zinc-blende and wurtzite has been extensively studied and well established in the past [8–10]. It is generally believed that the hexagonal phase has a larger band gap than the cubic phase and they form a type-II band alignment with the hexagonal phase having both higher valence band maximum (VBM) and conduction band minimum (CBM). Here, we raise the question of whether the understanding of the relationship between the zinc-blende and wurtzite band structures can be *transferred* to the case of diamond and lonsdaleite structures in the elemental semiconductors.

In this work, using first-principles calculations, we study and compare the electronic band structures of Ge in 3*C* and 2*H* phases and compare that with a II–VI compound ZnSe, of which both the cation and anion belong to the same row as Ge in the Periodic Table. For the analysis, we simultaneously consider the zone folding, crystal-field splitting, and the symmetry-controlled energy level repulsion effects. Not only do our results provide a thorough energy level correspondence between the 3*C* and 2*H* phases in Ge and ZnSe, but they also explain the origin of the different band alignment types between Ge and ZnSe. The concepts herein could be readily extended to other crystal systems in the presence and absence of inversion symmetry. Moreover, we propose that 2*H*-Ge can be stabilized by introducing electrons into the cubic ground state because the 2*H* phase has a much lower CBM than the 3*C*-Ge. This idea has been supported by our calculation of total energy difference and is distinct from that in zinc-blende semiconductors.

II. COMPUTATIONAL METHOD

Our first-principles calculations are carried out using the projector augmented wave (PAW) method [11] and density

*hxdeng@semi.ac.cn
†suhuaiwei@csrc.ac.cn

245202-1

TABLE I. Calculated lattice parameters (a and c) and band gap (E_g) of Ge and ZnSe in both $3C$ cubic and $2H$ hexagonal forms. Experimental values for lattice parameters and band gaps are listed in the parentheses. The space group and point group for each structure are also given.

	Diamond $3C$-Ge	Lonsdaleite $2H$-Ge	Zinc-blende $3C$-ZnSe	Wurtzite $2H$ ZnSe
Space group	$Fd\bar{3}m$	$P6_3mmc$	$F\bar{4}3m$	$P6_3mc$
Point group	O_h^7	D_{6h}^4	T_d^2	C_{6v}^4
a (Å)	5.670 (5.658[a])	3.995 (3.960[b])	5.665 (5.667[c])	3.982 (3.970[d])
c (Å)		6.592 (6.570[b])		6.548 (6.520[d])
E_g (eV)	0.669 (0.744[e])	0.307 (0.350[f])	2.712 (2.822[c])	2.751 (2.874[g])

[a]Reference [22].
[b]Reference [23].
[c]Reference [24].
[d]Reference [25].
[e]Reference [26].
[f]Reference [6].
[g]Reference [27].

functional theory (DFT) [12,13] as implemented in the VASP code [14,15]. We use a cutoff energy of 500 eV for the plane-wave basis set. The revised Perdew-Burke-Ernzerhof for solids (PBEsol) generalized gradient approximations [16] are adopted for structure optimization with a convergence criterion of 0.01 eV/Å for the Hellmann-Feynman force on each atom. The Brillouin zone of cubic and hexagonal lattices are sampled with Γ-centered $12 \times 12 \times 12$ and $12 \times 12 \times 6$ Monkhorst–Pack k mesh, respectively. As shown in Table I, the calculated lattice parameters for Ge and ZnSe in both $3C$ and $2H$ phases are all in good agreement with available experimental values. Subsequently, to reproduce the reliable electronic band structures for these semiconductors, we employ a modified Becke and Johnson exchange potential (mBJ) method [17] in the light of its validated accuracy in studying the electronic properties for various materials [18]. The obtained fundamental band gaps are in line with the experimental measurements (see Table I). We also list the space group and point group for each structure in Table I. The irreducible representations of the Bloch wave functions are determined by performing DFT calculations as implemented in QUANTUM ESPRESSO [19,20]. Note that we consider both cases with and without spin-orbit coupling in our electronic structure calculations and symmetry determinization for the sake of capturing a clear picture of the electronic features. The HSE06 screened hybrid density functional [21] with Hartree-Fock exchange parameter $\alpha = 0.25$ is employed to study the effect of charging, for which the use of the mBJ functional has not been well established.

The band alignment between the cubic $3C$ phase and its hexagonal $2H$ counterpart for a material (Ge or ZnSe) is calculated using the standard band offset calculation method described in Ref. [28]. The valence band offset between two forms $3C$ and $2H$ is given by

$$\Delta E_V(3C - 2H) = (E_V - E_{CL})_{2H} - (E_V - E_{CL})_{3C} + \Delta E_{CL}, \tag{1}$$

where $(E_V - E_{CL})_{2H}$ and $(E_V - E_{CL})_{3C}$ are the energy difference between the valence band maximum (VBM) and the core level for bulk $3C$ and $2H$ phases, respectively, and ΔE_{CL}

refers to the core-level binding energy separations for $3C$ and $2H$ phases in the corresponding $3C/2H$ heterojunction, of which the lattice constants are taken as the average ones of the $3C$ and $2H$ layers. The atomic positions of the superlattice are fully relaxed with a Γ-centered $12 \times 12 \times 1$ grid.

III. RESULTS AND DISCUSSION

The irreducible Brillouin zones (BZs) and high symmetry k points of face-centered-cubic (fcc) and primitive hexagonal (hex) phases, respectively, corresponding to the $3C$ and $2H$ structures are illustrated in Figs. 1(a) and 1(b). For better distinguishing the two phases, here we adopt an overbar for the high symmetry state in the $2H$ structure. The space group of $2H$ hexagonal structure is not the subgroup of the $3C$ cubic structure, so no exact k-point folding relationship exists at a general k point between the two structures. Nevertheless, an intimate folding relevance for the symmetry points in the Brillouin zone exists going from $3C$ to $2H$ phases. Perhaps this relationship can be best understood by virtue of the direct mapping between the $3C$ symmetry line Γ-L$^\perp$ [where L$^\perp$ refers to the L points along the $3C$ (111) axis] and the $\bar{\Gamma}$-$\bar{A}$ line in $2H$ hexagonal structure. Specifically, both the high symmetry points Γ and L$^\perp$ in the $3C$ cubic zone are folded onto the $2H$ $\bar{\Gamma}$ point. Aside from this folding relationship, there is an approximate connection between the BZ symmetry point of $3C$ and $2H$ structures. The X and L$^\parallel$ (where L$^\parallel$ represents the rest three L points except L$^\perp$) points in the cubic zone will be mapped onto the $2H$ $\bar{U}$ point, which lies on the $\bar{M} - \bar{L}$ line with the $\bar{M}$-$\bar{U}$/$\bar{U}$-$\bar{L}$ distance ratio of 2.0 [29]. Accordingly, the energy eigenvalue at the $2H$ $\bar{U}$ point is nearly the average of energies of X and L points in the cubic phase.

Figures 1(c)–1(f) depict the calculated electronic band structures without spin-orbit coupling for the diamond and lonsdaleite Ge, as well as the zinc-blende and wurtzite ZnSe. The irreducible representations of band states are given for the Γ and L points in $3C$, and the $\bar{\Gamma}$ point in $2H$ structures. From the symmetry perspective, the primary distinctive feature between Ge and ZnSe is that both cubic and
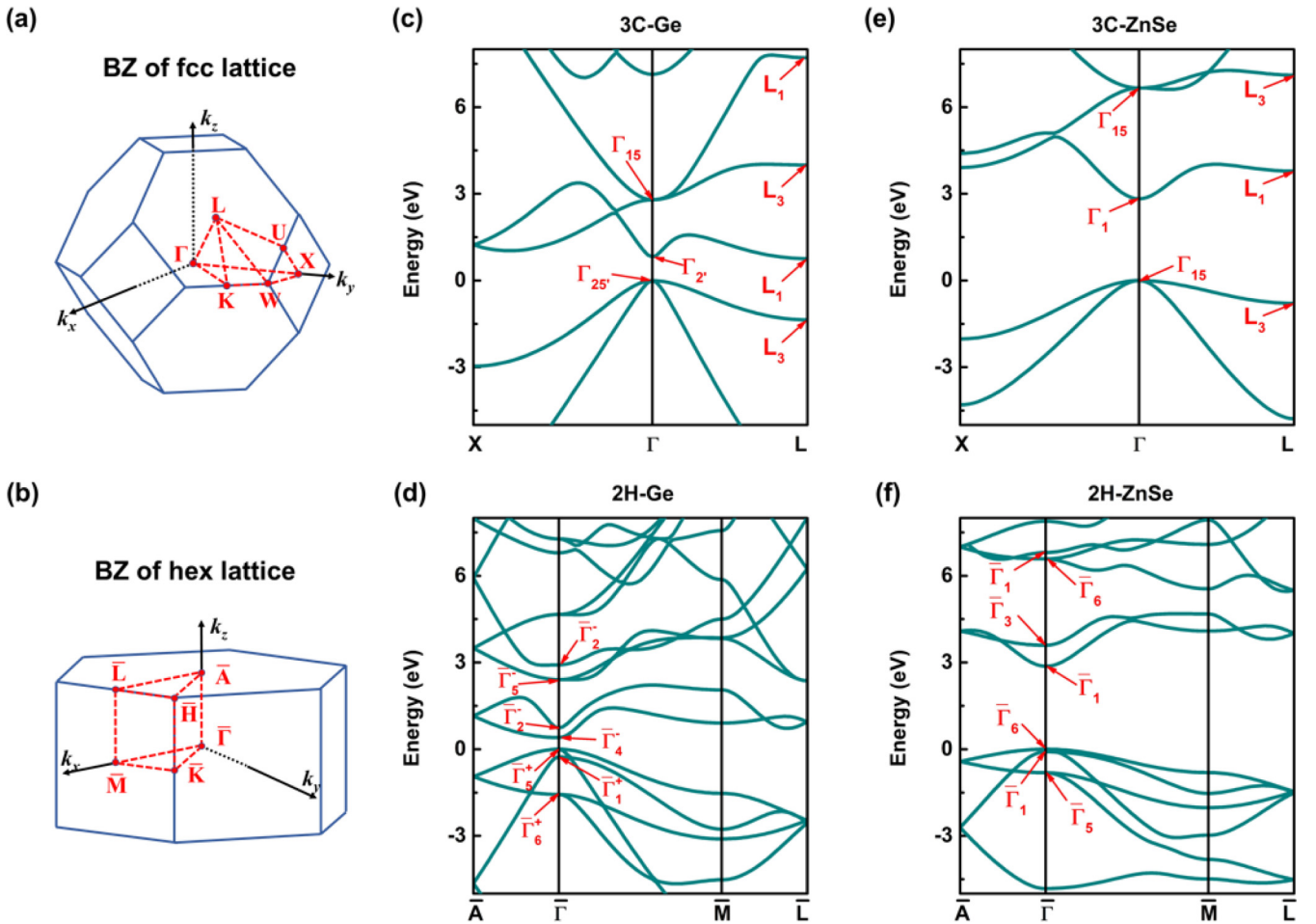
FIG. 1. First Brillouin zones and corresponding high symmetry points shown in red for (a) 3C cubic, and (b) 2H hexagonal crystals. The band structures for (c) 3C -Ge and (e) 3C -ZnSe along X-Γ-L high-symmetry path, and (d) 2H -Ge and (f) 2H -ZnSe along $\bar{A} - \bar{\Gamma} - \bar{M} - \bar{L}$ high-symmetry path. The VBM is set at energy zero. The single-group irreducible representations [30] of band states at the Γ and L points in 3C, and the $\bar{\Gamma}$ point in 2H structures are indicated. The superscript $+$ $(-)$ of the irreducible representation denotes the even- (odd-) parity band state for system with inversion symmetry.

hexagonal Ge structures have the inversion symmetry, which is absent for ZnSe in both phases. The inversion-induced even- (odd-)parity of the band state for Ge is clearly marked with superscript $+$ $(-)$ in the corresponding irreducible representation. The relevant 3C band states are mapped onto the 2H structure as discussed above. Going from 3C to 2H for both Ge and ZnSe, the number of 2H bands are doubled at each k point since the 2H primitive cell possesses twice as many atoms as the 3C cubic cell. It is noted that the band gap of ZnSe is direct at the Γ point in both cubic and hexagonal phases, and 2H-ZnSe ($E_g \sim 2.751$ eV) has a slightly larger fundamental band gap than its cubic counterpart ($E_g \sim 2.712$ eV). Unlike ZnSe, the fundamental band gap of 3C-Ge is indirect with the VBM at Γ and CBM at L, which is 0.058 eV lower than that at Γ, while 2H-Ge turns out to be a pseudodirect band gap crystal. The band gap of 2H-Ge ($E_g \sim 0.307$ eV) is remarkably smaller than that of 3C-Ge ($E_g \sim 0.669$ eV).

Moreover, our band offset calculations reveal that Ge and ZnSe have different types of band alignment: the former one displays the straddling type I, while the latter one is of the

staggered type II. For the case of ZnSe, both the VBM and CBM of the 3C phase are lower in energy than that of the 2H phase by $\sim$0.047 and $\sim$0.086 eV, respectively. This trend actually falls in line with the common wisdom on the band offset between the wurtzite and zinc-blende structures [31,32]. As for Ge, we observe that the 3C VBM is $\sim$0.162 eV lower than that of the 2H phase, while the 3C CBM has a $\sim$0.200 eV higher CBM compared with the 2H structure.

In what follows, to examine the electronic structure properties of the two cases more intuitively and closely, we examine the energy levels involved in the vicinity of the band gap edges going from 3C to 2H phases for both Ge and ZnSe, considering the band folding arguments, crystal-field splitting, together with symmetry-controlled level repulsion effects (see Fig. 2).

(i) *The nature of the elevated 2H VBM states.* The 2H hexagonal crystal field splits the 3C VBM at the Γ point into two states, namely from $\Gamma'_{25v} \rightarrow \bar{\Gamma}^+_{5v}$ and $\bar{\Gamma}^+_{1v}$ for Ge and from $\Gamma_{15v} \rightarrow \bar{\Gamma}_{6v}$ and $\bar{\Gamma}_{1v}$ for ZnSe. As indicated in Fig. 2, the spin-orbit coupling further splits the valence band states and gives rise to the normal decreasing energy ordering of
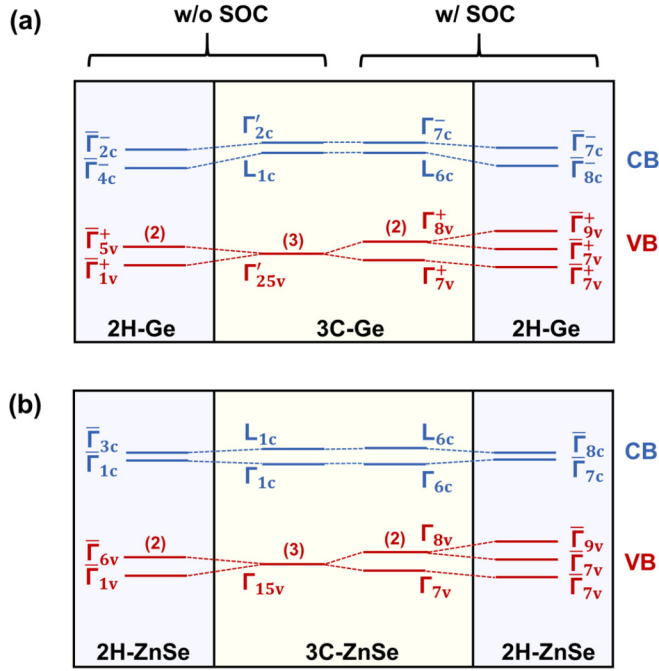
FIG. 2. The schematic energy-level-correspondence diagram of selected levels at the L and Γ points of cubic structure (central yellow panel) and $\bar{\Gamma}$ point of hexagonal structure (left and right purple panel) with or without spin-orbit coupling (w/ or w/o SOC) effects for (a) Ge and (b) ZnSe semiconductors. The values in parentheses above the band states represents the degeneracy of the energy levels. CB (VB) indicates the conduction (valence) bands specified by subscript $c(v)$ in the irreducible representations.

FIG. 3. The energy difference between the cubic and the hexagonal structures for Ge and ZnSe as a function of the carrier density in units of per two-atom formula. The slopes (k) are 0.035 for Ge with electron injection, 0.023 for Ge with hole injection, and 0.005 for ZnSe with hole injection.

$\bar{\Gamma}_{9v} > \bar{\Gamma}_{7v} > \bar{\Gamma}_{7v}$ (for systems with positive SOC and crystal field splitting, and all with even-parity in Ge) for the top three valence bands in the $2H$ phase. In short, it is the crystal-field splitting that leads to the higher VBM level for $2H$ than that of $3C$ cubic in both Ge and ZnSe. The larger valence band offset in Ge compared to ZnSe can be partly ascribed to its larger c/a ratio of $\sim$1.650 than that of ZnSe ($c/a = 1.644$), which leads to a larger crystal field splitting.

(ii) *The nature of the raised and lowered CBM.* $3C$-ZnSe is a direct band gap semiconductor with both CBM and VBM located at the Γ point. The split valence state $\bar{\Gamma}_{1v}$ ($\bar{\Gamma}_{7v}$) couples with the $\bar{\Gamma}_{1c}$ ($\bar{\Gamma}_{7c}$) CBM in the $2H$ structure thus making the CBM in $2H$-ZnSe higher than that of its $3C$ counterpart, while the band gap of $3C$-Ge is indirect with its CBM at L_{1c} (L_{6c}), slightly below the band energy at Γ'_{2c} (Γ^-_{7c}). Given the zone folding analysis, it is found that the $L^\perp_{1c}$ ($L^\perp_{6c}$) is folded into the $\bar{\Gamma}^-_{4c}$ ($\bar{\Gamma}^-_{8c}$) state going from $3C$ to $2H$. Accodingly, there is a strong repulsion between the folded CBM orbital $\bar{\Gamma}^-_{4c}$ ($\bar{\Gamma}^-_{8c}$) and a higher state folded from the second lowest $L^\perp_{1c}$ ($L^\perp_{6c}$) orbital in $3C$ cubic, leading to the downwards shift of CBM in $2H$ with respect to the $3C$ phase. Unlike in $2H$-ZnSe, due to the higher symmetry, there is no internal VB-CB level repulsion in the $2H$-Ge. Note that even taking the SOC effect into account, the split valence state $\bar{\Gamma}^+_{7v}$ will not interact with the conduction state $\bar{\Gamma}^-_{7c}$ because of their different parities pertained to the inversion symmetry.

As a result of the symmetry analysis, we can conclude that although the diamond (lonsdaleite) structure resembles

the zinc-blende (wurtzite) structure, it is improper to simply transfer the previous well-established picture of energy level relationship between the zinc-blende and wurtzite phases [8–10] to that of diamond and lonsdaleite. Specifically, the inter-VB-CB level repulsion dominates in the compound without inversion symmetry, whereas it vanishes in the elemental semiconductors because of the existence of inversion symmetry and the intra-CB level repulsion becomes more important.

It is quite desirable to stabilize the hexagonal phase of Ge due to its direct band gap. In principle, a phase equiped with lower CBM (higher VBM) will gain more energy after adding electrons (holes). Accordingly, the observation and analysis on the $3C/2H$ band alignment suggest to us that it could be feasible to stabilize the metastable phase of Ge by incorporating the electrons or holes into the Ge, whereas for hexagonal ZnSe, it can only be stabilized by holes [31,32]. To test this idea, as shown in Fig. 3, we calculate the energy difference between the cubic and the hexagonal structures for Ge versus the injected carrier density in units of carriers per formula. For ZnSe, we only portray the case of hole injection. The negative $\Delta E(3C$-$2H)$ values at carrier density of zero clearly point out that the most stable phases for Ge and ZnSe are both the $3C$ cubic phases. As electrons or holes are incorporated, the energy difference gradually becomes less negative and will finally become positive at some point; namely, the $2H$ hexagonal phase is stabilized. Since the VBM of $2H$-ZnSe is only slightly above the $3C$-ZnSe by $\sim$0.047 eV, the slope is found to be very small. For Ge, the slope with introduced electrons is larger than that with introduced holes due to the larger CBM offset compared with the VBM offset; that is, it is easier to stabilize the $2H$-Ge by adding electrons.

IV. CONCLUSION

In conclusion, we have carried out first-principles calculations to investigate the $3C$ and $2H$ electronic band structures of Ge and ZnSe. The energy level relationship between the

$3C$ and $2H$ phases in Ge is carefully analyzed and compared with that of ZnSe considering the crystal-field splitting, band folding, as well as symmetry-controlled band coupling effects. We find that the internal VB-CB level repulsion exists in the wurzite structure, but vanishes in the lonsdaleite structure due to the presence of inversion symmetry in the elementary semiconductor, which explains the different $3C/2H$ band alignment types between Ge and ZnSe. More importantly, based on the fact that hexagonal Ge has a much lower CBM compared to its cubic structure, we demonstrate that the direct band gap $2H$-Ge can be stabilized by incorporating electrons into the $3C$-Ge.

[1] D. Thomson, A. Zilkie, J. E. Bowers, T. Komljenovic, G. T. Reed, L. Vivien, D. Marris-Morini, E. Cassan, L. Virot, and J.-M. Fédéli, Roadmap on silicon photonics, J. Opt. **18**, 073003 (2016).

[2] P. Cheben, R. Halir, J. H. Schmid, H. A. Atwater, and D. R. Smith, Subwavelength integrated photonics, Nature (London) **560**, 565 (2018).

[3] C. Frondel and U. B. Marvin, Lonsdaleite, a hexagonal polymorph of diamond, Nature (London) **214**, 587 (1967).

[4] A. De and C. E. Pryor, Electronic structure and optical properties of Si, Ge and diamond in the lonsdaleite phase, J. Phys.: Condens. Matter **26**, 045801 (2014).

[5] C. Rödl, J. Furthmüller, J. R. Suckert, V. Armuzza, F. Bechstedt, and S. Botti, Accurate electronic and optical properties of hexagonal germanium for optoelectronic applications, Phys. Rev. Materials **3**, 034602 (2019).

[6] E. M. T. Fadaly, A. Dijkstra, J. R. Suckert, D. Ziss, M. A. J. van Tilburg, C. Mao, Y. Ren, V. T. van Lange, K. Korzun, S. Kolling, M. A. Verheijen, D. Busse, C. Rodl, J. Furthmuller, F. Bechstedt, J. Stangl, J. J. Finley, S. Botti, J. E. M. Haverkort, and E. Bakkers, Direct-bandgap emission from hexagonal Ge and SiGe alloys, Nature (London) **580**, 205 (2020).

[7] C. Raffy, J. Furthmüller, and F. Bechstedt, Properties of hexagonal polytypes of group-IV elements from first-principles calculations, Phys. Rev. B **66**, 075201 (2002).

[8] C.-Y. Yeh, Z. Lu, S. Froyen, and A. Zunger, Zinc-blende–wurtzite polytypism in semiconductors, Phys. Rev. B **46**, 10086 (1992).

[9] C.-Y. Yeh, S.-H. Wei, and A. Zunger, Relationships between the band gaps of the zinc-blende and wurtzite modifications of semiconductors, Phys. Rev. B **50**, 2715 (1994).

[10] L. L. Y. Voon, M. Willatzen, M. Cardona, and N. Christensen, Terms linear in k in the band structure of wurtzite-type semiconductors, Phys. Rev. B **53**, 10703 (1996).

[11] G. Kresse and D. Joubert, From ultrasoft pseudopotentials to the projector augmented-wave method, Phys. Rev. B **59**, 1758 (1999).

[12] W. Kohn and L. J. Sham, Self-consistent equations including exchange and correlation effects, Phys. Rev. **140**, A1133 (1965).

[13] W. Kohn, A. D. Becke, and R. G. Parr, Density functional theory of electronic structure, J. Phys. Chem. **100**, 12974 (1996).

[14] G. Kresse and J. Furthmüller, Efficient iterative schemes for ab initio total-energy calculations using a plane-wave basis set, Phys. Rev. B **54**, 11169 (1996).

[15] G. Kresse and J. Furthmüller, Efficiency of ab-initio total energy calculations for metals and semiconductors using a plane-wave basis set, Comput. Mater. Sci. **6**, 15 (1996).

[16] J. P. Perdew, A. Ruzsinszky, G. I. Csonka, O. A. Vydrov, G. E. Scuseria, L. A. Constantin, X. Zhou, and K. Burke, Restoring the Density-Gradient Expansion for Exchange in Solids and Surfaces, Phys. Rev. Lett. **100**, 136406 (2008).

[17] A. D. Becke and E. R. Johnson, A simple effective potential for exchange, J. Chem. Phys. **124**, 221101 (2006).

[18] Y.-S. Kim, M. Marsman, G. Kresse, F. Tran, and P. Blaha, Towards efficient band structure and effective mass calculations for III-V direct band-gap semiconductors, Phys. Rev. B **82**, 205212 (2010).

[19] P. Giannozzi, S. Baroni, N. Bonini, M. Calandra, R. Car, C. Cavazzoni, D. Ceresoli, G. L. Chiarotti, M. Cococcioni, and I. Dabo, QUANTUM ESPRESSO: A modular and open-source software project for quantum simulations of materials, J. Phys.: Condens. Matter **21**, 395502 (2009).

[20] P. Giannozzi, O. Andreussi, T. Brumme, O. Bunau, M. B. Nardelli, M. Calandra, R. Car, C. Cavazzoni, D. Ceresoli, and M. Cococcioni, Advanced capabilities for materials modelling with Quantum ESPRESSO, J. Phys.: Condens. Matter **29**, 465901 (2017).

[21] J. Heyd, G. E. Scuseria, and M. Ernzerhof, Hybrid functionals based on a screened Coulomb potential, J. Chem. Phys. **118**, 8207 (2003).

[22] A. Smakula and J. Kalnajs, Precision determination of lattice constants with a Geiger-counter x-ray diffractometer, Phys. Rev. **99**, 1737 (1955).

[23] S. Xiao and P. Pirouz, On diamond-hexagonal germanium, J. Mater. Res. **7**, 1406 (1992).

[24] W. Stutius, Growth and doping of ZnSe and ZnS_xSe_{1-x} by organometallic chemical vapor deposition, J. Cryst. Growth **59**, 1 (1982).

[25] B. Xi, S. Xiong, D. Xu, J. Li, H. Zhou, J. Pan, J. Li, and Y. Qian, Tetraethylenepentamine-directed controllable synthesis of wurtzite ZnSe nanostructures with tunable morphology, Chem. - Eur. J. **14**, 9786 (2008).

[26] S. Zwerdling, B. Lax, L. M. Roth, and K. J. Button, Exciton and magneto-absorption of the direct and indirect transitions in germanium, Phys. Rev. **114**, 80 (1959).

[27] M. Oshikiri and F. Aryasetiawan, Band gaps and quasiparticle energy calculations on ZnO, ZnS, and ZnSe in the zinc-blende structure by the GW approximation, Phys. Rev. B **60**, 10754 (1999).

[28] S. H. Wei and A. Zunger, Valence band splittings and band offsets of AlN, GaN, and InN, Appl. Phys. Lett. **69**, 2719 (1996).

[29] M. R. Salehpour and S. Satpathy, Comparison of electron bands of hexagonal and cubic diamond, Phys. Rev. B **41**, 3048 (1990).

[30] G. Roster, J. Dimmock, R. Wheeler, and H. Statz, *Properties of the Thirty-Two Point Groups* (MIT, Cambridge, MA, 1963), Vol. 24.

[31] G. M. Dalpian and S.-H. Wei, Hole-Mediated Stabilization of Cubic GaN, Phys. Rev. Lett. **93**, 216401 (2004).

[32] G. M. Dalpian, Y. Yan, and S.-H. Wei, Impurity-induced phase stabilization of semiconductors, Appl. Phys. Lett. **89**, 011907 (2006).